A&A 475, 375–389 (2007)
DOI: 10.1051/0004-6361:20077979

Astronomy & Astrophysics

Collisional and dynamical evolution of the L_4 Trojan asteroids

G. C. de Elía and A. Brunini

Facultad de Ciencias Astronómicas y Geofísicas, Universidad Nacional de La Plata, Paseo del Bosque S/N (1900), La Plata, Argentina
IALP-CONICET, Argentina
e-mail: [gdeelia;abrunini]@fcaglp.unlp.edu.ar

Received 30 May 2007 / Accepted 7 September 2007

ABSTRACT

Aims. In this paper, we analyze the collisional and dynamical evolution of the population of L_4 Jovian Trojans.
Methods. To do this, we test different collisional parameters and include a dynamical treatment, taking into account the stability and instability zones of the L_4 Trojan swarm. This procedure allows us to estimate the size distribution of the L_4 Trojans, to study their mean collisional lifetimes, to analyze the formation of families, to obtain ejection rates of Trojan fragments and to discuss their possible contribution to the current populations of Centaurs and Jupiter-family comets.
Results. Our estimates of the L_4 Trojan cumulative size distribution show waves that propagate from diameters of ~0.1 to ~80 km around the values derived from optical surveys. On the other hand, the mean collisional lifetimes obtained from our simulations indicate that the large Trojan asteroids have likely survived without being catastrophically fragmented over the age of the Solar System. With regards to the Trojan removal, we calculate a maximum ejection rate of Trojan fragments from L_4 of ~50 objects larger than 1 km of diameter per Myr, which results to be significantly smaller than values previously published. Such estimates allow us to infer that the contribution of the Trojan asteroids to the current populations of Centaurs and Jupiter-family comets is negligible. In addition, our results are in agreement with the formation of few Trojan families in the L_4 swarm. On the other hand, we infer that the current orbital distribution of the Trojan asteroids does not offer a strong constraint on the dynamical origin of this population.

Key words. minor planets, asteroids – methods: numerical – solar system: formation

1. Introduction

The Jovian Trojan asteroids are objects locked in a 1:1 mean motion resonance with Jupiter, which lead and trail the planet by 60 degrees of longitude, librating around the Lagrangian equilibrium points L_4 and L_5. While the possible existence of objects moving on stable orbits in the vicinity of such equilibrium points was demonstrated by Joseph-Louis Lagrange more than two centuries ago (Lagrange 1772), such asteroids were not discovered until the early 1900s. In fact, in 1906, Max Wolf observed the first Jovian Trojan librating around the L_4 point while a second body was found orbiting L_5 by August Kopff the same year. Designated as (588) Achilles and (617) Patroclus, respectively, these asteroids represented an observational confirmation of Lagrange's studies about the triangular equilibrium points in the restricted three-body problem.

The first comprehensive works aimed at understanding the dynamical properties of the Trojan asteroids in the frame of the restricted three-body problem were developed by Szebehely (1967) and Rabe (1967). In fact, Szebehely (1967) performed a detailed description of such problem including regularization, equilibrium points, periodic orbits and their stability, Hill curves and their implications. At the same time, Rabe (1967) studied the long-period Trojan librations and defined the stability limits in the eccentricity-libration amplitude space. Some years later, Érdi (1978) analyzed analytically the three-dimensional motion of the Trojan asteroids within the framework of the elliptic restricted three-body problem and investigated the main perturbations of Jupiter in the orbital elements. On the other hand, the dynamical behavior of the Jupiter Trojan populations has been also widely studied by numerical methods. Based on a sample of 40 Trojans, Bien & Schubart (1987) described the construction of three proper elements for the Trojan asteroids – the amplitude of libration, the proper eccentricity and the proper inclination – which were shown to be constants over some 10^5 yr, at least. Later, Schubart & Bien (1987) analyzed the distribution of these quantities and their relation to other dynamical parameters. In the early 1990s, Milani (1993) numerically integrated the orbits of 174 asteroids in the 1:1 resonance with Jupiter for 1 Myr taking into account the gravitational influence of the four giant planets. This work was capable of computing accurate and stable proper elements for the sample of Trojans, allowing to detect some significant candidate asteroid families. Later, Levison et al. (1997) developed long-term dynamical integrations in order to study the stability of the Trojan asteroids under the perturbations of all the outer planets over long timescales of $\sim 10^9$ yr. Using a full N-body model, Levison et al. (1997) showed that the Trojans move on orbits which are not stable indefinitely, indicating that the gravitational influence of the giant planets has reduced the outer boundaries of the swarms over time. In fact, the most important result obtained by these authors is that the Trojan clouds of Jupiter are slowly dispersing, estimating a dynamical erosion rate of $\sim 6.2 \times 10^{-5}$ yr^{-1} objects with diameters greater than 1 km from the swarms.

Another important question concerning Trojan asteroids is their collisional history. The first attempt to study the collisional

evolution of these objects was made by Davis & Weidenschilling (1981) who derived results regarding mean impact velocities and mean intervals between catastrophic collisions for different size Trojan asteroids. In fact, these authors found a mean collision speed for Trojans of approximately 3.5 km s^{-1} based on a set of only 69 objects. On the other hand, they suggested that the larger Trojan asteroids represent a part of the population which has likely survived unaltered by catastrophic impacts over the age of the Solar System.

Armed with accurate proper elements of a sample of 174 Trojans, Milani (1993, 1994) identified 3 reliable families: the Menelaus and Teucer families in the L_4 swarm, and the Sarpedon family in L_5. The existence of these families and smaller asteroid clusters allowed to confirm the occurrence of significant collisional evolution in the Trojan swarms. Later, Marzari et al. (1995) studied the formation of Trojan collisional families and analyzed a possible connection between the fragments yield in the Trojan clouds and the population of short-period comets. In fact, these authors showed that ~20% of these fragments end up into unstable orbits having close encounters with Jupiter and suggested that a few tens of the observed short-period comets might have been originated by collisions in the Trojan swarms.

In the second half 1990s, Marzari et al. (1996) developed a numerical approach aimed at calculating collision rates and impact velocities for Trojan asteroids. Based on a set of 114 Trojans, these authors computed the values of these collisional parameters over a short timescale of $\sim 10^4$ yr, estimating average intrinsic collision probabilities for the L_4 and L_5 swarms, and a mean collision speed of approximately 5 km s^{-1}, which is a little more higher compared to that derived by Davis & Weidenschilling (1981). Using these collisional parameters and energy scaling of impact strength with size, Marzari et al. (1997) modeled the collisional evolution of the Trojan asteroids. They predicted the formation of several tens of Trojan families generated by the breakup of parent bodies larger than 60 km and suggested that the flux of fragments ending up into Jupiter-crossing cometary orbits could supply ~10% of the population of short-period comets and Centaur asteroids. Later, Dell'Oro et al. (1998) developed a statistical method aimed at computing the collision probability and the impact velocity in the two Trojan clouds over a longer timescale than that used by Marzari et al. (1996) (~1 Myr), allowing to account for the dynamical links among the Trojans and Jupiter orbital angles due to the 1:1 resonance. Based on a set of 223 Trojans, Dell'Oro et al. (1998) estimated average intrinsic collision probabilities for the L_4 and L_5 swarms, and a mean collision speed of approximately 4.5 km s^{-1}.

In the early 2000s, Gil-Hutton & Brunini (2000) numerically simulated the collisional interaction between the outer asteroid belt and scattered primordial planetesimals from the Uranus-Neptune zone during their accretion period. They showed that the final size distributions of the Trojans and Hildas are dominated by the cometesimal bombardment, which happens during the first 2×10^7 yr of evolution (Brunini & Fernández 1999).

At the same time, Jewitt et al. (2000) presented a study of the population and size distribution of small Jovian Trojan asteroids developed from an optical survey taken in the direction of the L_4 swarm. These authors estimated that the number of L_4 Trojans with radius larger than 1 km is about 1.6×10^5. Moreover, they argued that a critical radius $r_c \sim 30$ to 40 km may mark a transition size between primordial objects and collisional fragments produced from larger bodies. Some years later, Yoshida & Nakamura (2005) detected 51 faint Jovian Trojan asteroids in the L_4 swarm corresponding to the diameter range of $0.7 \leq D \leq 12.3$ km. These authors calculated the Trojan size distribution in the size range of $2 \leq D \leq 10$ km and, for this entire range, they found results consistent with those previously derived by Jewitt et al. (2000). However, Yoshida & Nakamura (2005) noted a slight break in the size distribution at $D \sim 5$ km, which, taken together with the results of Jewitt et al. (2000), may suggest that the global Trojan size distribution has a continuously changing slope.

On the other hand, Beaugé & Roig (2001) performed a semi-analytical model for the motion of the Trojan asteroids aimed at studying the dynamical behavior of these bodies over long timescales. Making use of this algorithm, these authors estimated accurate proper elements for a sample of 533 Trojans, which allowed them to search for asteroid families among the L_4 and L_5 swarms. In fact, while Beaugé & Roig (2001) confirmed the existence of the Menelaus family around L_4, previously detected by Milani (1993, 1994), they put in doubt Milani's (1993, 1994) Teucer family, proposing the Epeios family as a more reliable candidate to be the byproduct of the breakup of a larger body. Moreover, Beaugé & Roig (2001) did not identify significant candidate families around L_5, suggesting a possible asymmetry between the two swarms. Some years later, Fornasier et al. (2004), Dotto et al. (2006) and Fornasier et al. (2007) carried out spectroscopic and photometric surveys of Trojan asteroids aimed at analyzing the mineralogical properties of small and large members of different dynamical families in order to investigate the nature of these groups and the internal composition of their parent bodies. In fact, making use of the list of Jupiter Trojan families provided by Beaugé & Roig (2001), Fornasier et al. (2004) developed a visible spectroscopic and photometric survey of the L_5 swarm, studying the properties of several members belonging to the Aneas, Astyanax, Sarpedon and Phereclos families. On the other hand, Dotto et al. (2006) performed a visible and near-infrared survey of the L_4 and L_5 swarms, investigating the surface properties of several members belonging to seven dynamical families of both clouds. In fact, these authors concentrated on the same four L_5 families studied by Fornasier et al. (2004) and analyzed the Menelaus, 1986 WD and Makhaon families in L_4. The most important result derived by Dotto et al. (2006) is the uniformity of the Trojan population. Recently, Fornasier et al. (2007) presented final results on dynamical families from a visible survey of L_4 and L_5 Trojans. These authors studied the main characteristics of small and large members of the Aneas, Anchises, Misenus, Phereclos, Sarpedon and Panthoos L_5 families and the Eurybates, Menelaus, 1986 WD and 1986 TS6 families in the L_4 cloud.

In this paper, we present a new study aimed at analyzing the collisional and dynamical evolution of the L_4 Trojan asteroids, using the numerical code developed by de Elía & Brunini (2007). While this paper is similar to that made by Marzari et al. (1997), there are relevant differences in the general treatment of the algorithm. As for the collisional model, Marzari et al. (1997) implemented three different Q_S laws (namely, the amount of energy per unit target mass needed to catastrophically fragment a body, such that the largest resulting fragment has half the mass of the original target, regardless of reaccumulation of fragments) formulated by Davis et al. (1985) (simple energy scaling), Housen & Holsapple (1990) (strain-rate scaling) and Davis et al. (1994) (hydrocode scaling), and assumed a constant value of 0.2 for factor f_{ke}, which determines the fraction of the energy received by a body released as kinetic energy of the fragments. Here, we use different Q_S laws and a factor f_{ke} depending on target size (Davis et al. 1995; O'Brien & Greenberg 2005) which are combined to yield the Q_D law (namely, the amount of energy per unit mass

needed to fragment a body and disperse half of its mass) formulated by Benz & Asphaug (1999) for icy targets and 3 km s^{-1} impact velocity. On the other hand, we believe our model improves that presented by Marzari et al. (1997), including a dynamical treatment that takes into account the stability and instability regions of the L_4 Trojan swarm, which allows us to obtain more reliable estimates about the collisional ejection rates of Trojan fragments, and to discuss their possible contribution to the current populations of Centaurs and Jupiter-family comets.

In Sect. 2 the collisional model is described, while the major dynamical features present in the L_4 Trojan population are discussed in Sect. 3. In Sect. 4 we describe the full numerical model. Section 5 shows the most important results derived from the collisional and dynamical evolution of the L_4 Trojan asteroids. Conclusions are given in the last section.

2. Collisional mechanisms

In this section, we give a brief description of the collisional algorithm developed by de Elía & Brunini (2007) aimed at describing the outcome of a collision between two bodies. Such algorithm is based on the method performed by Petit & Farinella (1993) with the corrections made by O'Brien & Greenberg (2005).

2.1. Collisional parameters – definitions

A catastrophic collision is defined as the one where the largest piece resulting from it contains 50% or less of the initial target mass, whereas the rest of the collisions are considered cratering events. When a collision between two bodies of masses M_1 and M_2 occurs, the relative kinetic energy is given by

$$E_{\rm rel} = \frac{1}{2}\frac{M_1 M_2}{M_1 + M_2} V^2, \tag{1}$$

where V is the relative impact velocity. The impact velocity V and the shattering impact specific energy Q_S are two fundamental quantities determining, for a given body, if the collision must be studied in the catastrophic regime or in the cratering regime. Farinella et al. (1982), Housen & Holsapple (1990), Ryan (1992), Holsapple (1993), Housen & Holsapple (1999) and Benz & Asphaug (1999) have shown that for small bodies, with diameters $\lesssim$1 km, the material properties control the impact strength in such a way that it decreases with increasing size. On another hand, Davis et al. (1985), Housen & Holsapple (1990), Love & Ahrens (1996), Melosh & Ryan (1997), and Benz & Asphaug (1999) showed that for large asteroids, with diameters $\gtrsim$1 km, gravity dominates the impact strength which increases with increasing size. In fact, while asteroids with diameters $\lesssim$1 km are assumed to be in the "strength-scaled regime", larger bodies are in the "gravity-scaled regime". Some authors (Durda et al. 1998) have used the dispersing impact specific energy Q_D rather than Q_S, as primary input parameter in their collisional evolution models. For small bodies, the gravitational binding energy is negligible and owing to that Q_S and Q_D have the same value. For larger bodies, Q_D must be larger than Q_S, since gravity is important and can therefore impede the dispersal of fragments. In Sect. 4.4, we discuss some aspects of Q_S and Q_D, specifying the most convenient input parameters for our collisional evolution model.

According to these definitions and assuming that the energy is equi-partitioned between the two colliding bodies (Hartmann 1988), for body i fragmentation occurs if $E_{\rm rel} > 2Q_{S,i}M_i$ (Greenberg et al. 1978; Petit & Farinella 1993), while below this threshold, cratering happens. Thus, if two objects collide, the last relation allows us to determine if both of them will be catastrophically fragmented, if one will be cratered and the other will be catastrophically fragmented or if both will be cratered after the collision.

In the next subsections, we describe our treatment of a collision in the catastrophic regime as well as in the cratering regime. Besides, for any of the three mentioned outcomes, we also study the escape and reaccumulation processes of the resulting fragments, carrying out a previous determination of the escape velocity.

2.2. Catastrophic fragmentation

If a body of mass M_i is catastrophically fragmented, the mass of the largest resulting fragment will be given by $M_{{\rm max},i} = M_i f_{l,i}$, where $f_{l,i}$ is

$$f_{l,i} = \frac{1}{2}\left(\frac{Q_{S,i}M_i}{E_{\rm rel}/2}\right)^{1.24}, \tag{2}$$

according to the experimental results obtained by Fujiwara et al. (1977).

We define $N_i(\geq m)$ as the number of fragments of body i with a mass larger than m. $N_i(\geq m)$ has a discontinuity at $m = M_{{\rm max},i}$ since there is just one fragment of mass $M_{{\rm max},i}$ resulting from the catastrophic fragmentation of body i. So, if $\Theta(x)$ is the Heaviside step function (namely, $\Theta(x) = 0$ for $x < 0$ and $\Theta(x) = 1$ for $x \geq 0$), $N_i(\geq m)$ can be written as

$$N_i(\geq m) = B_i m^{-b_i}\Theta(M_{{\rm max},i} - m), \tag{3}$$

where b_i is the characteristic exponent. Besides, as $N_i(\geq M_{{\rm max},i}) = 1$, so from the last equation, we find $B_i = (M_{{\rm max},i})^{b_i}$. In order to calculate the characteristic exponent b_i, we derive the cumulative mass distribution $M_i(\leq m)$ which represents the total mass of fragments of body i with a mass smaller than m. In fact, $M_i(\leq m)$ can be calculated as

$$M_i(\leq m) = \int_0^m m n_i(m){\rm d}m, \tag{4}$$

where $n_i(m){\rm d}m = -{\rm d}N_i(\geq m)$ defines the differential fragment size distribution. Thus, $M_i(\leq m)$ will be written as

$$M_i(\leq m) = \frac{b_i M_{{\rm max},i}^{b_i}}{1-b_i} m^{1-b_i}\{1 - \Theta(m - M_{{\rm max},i})\} + \frac{M_{{\rm max},i}}{1-b_i}\Theta(m - M_{{\rm max},i}). \tag{5}$$

On the other hand, the mass conservation implies $M_i(\leq M_{{\rm max},i}) = M_i$; then, from Eq. (5), we derive the condition

$$M_i = \frac{M_{{\rm max},i}}{1-b_i}, \tag{6}$$

and, since $M_{{\rm max},i} = M_i f_{l,i}$, so

$$b_i = 1 - f_{l,i}. \tag{7}$$

Thus, if $f_{l,i}$ is calculated by Eq. (2), b_i can be derived from the last equation. With this, every parameter present in Eq. (3) is determined and so, such law can be used in order to calculate the distribution of the fragments resulting from a catastrophic event.

2.3. Cratering impacts

Below the catastrophic fragmentation threshold ($E_{\rm rel} < 2Q_{S,i}M_i$), a crater is formed. Imposing continuity for $M_{{\rm crat},i} = M_i/100$, the mass $M_{{\rm crat},i}$ excavated from the crater can be calculated from the following relations

$$M_{{\rm crat},i} = \begin{cases} \alpha E_{\rm rel} & \text{if } E_{\rm rel} \le \beta, \\ \dfrac{9\alpha}{200Q_{S,i}\alpha - 1}E_{\rm rel} + \dfrac{M_i}{10}\dfrac{1-20Q_{S,i}\alpha}{1-200Q_{S,i}\alpha} & \text{if } E_{\rm rel} > \beta, \end{cases} \quad (8)$$

where $\beta = M_i/100\alpha$. The parameter α, known as crater excavation coefficient, depends on the material properties and ranges from about 4×10^{-4} to 10^{-5} s^2 m^{-2} for soft and hard materials respectively (Stoeffler et al. 1975; Dobrovolskis & Burns 1984). For cratering impacts, the surviving cratered body has a mass $M_i - M_{{\rm crat},i}$. It is important to take into account that the derived expressions to treat a catastrophic impact can be used in order to study a cratering event, replacing the target mass M_i by $M_{{\rm crat},i}$. Thus, the mass of the largest fragment ejected from the crater will be $f_{l,i}M_{{\rm crat},i}$, where $f_{l,i} = 0.2$ since according to Melosh (1989), $b_i = 0.8$ for any cratering event.

2.4. Escape and reaccumulation of fragments

After calculating the distribution of fragments associated with every one of bodies that participate in a collision, it is necessary to determine the final fate of the fragments ejected from each one of them. If the fragment relative velocity is larger than the escape velocity $V_{\rm esc}$ from the two colliding bodies, it will escape, while those slower than $V_{\rm esc}$ will be reaccumulated on the largest remnant. The following points must be considered:

- to adopt a Fragment Velocity Distribution;
- to determine the Escape Velocity of the Fragments.

Here, we follow the method of Petit & Farinella (1993) to calculate the velocity distribution of fragments. The mass-velocity distribution can be written as

$$\begin{aligned} V &= C_i m^{-r_i} \quad \text{for} \quad \bar{M}_i \le m \le M_{{\rm max},i}, \\ V &= V_{\rm max} \quad \text{for} \quad m < \bar{M}_i, \end{aligned} \quad (9)$$

where, imposing continuity, $\bar{M}_i = (V_{\rm max}/C_i)^{-1/r_i}$. $V_{\rm max}$ is assumed to be the maximum value for the velocity of the fragments. The inclusion of this high velocity cutoff is motivated by a physical reason: a fragment can not be ejected with a velocity larger than the sound speed in the material, which is assumed to be of 3000 m s^{-1} (O'Brien & Greenberg 2005). While this value would seem to be too large (Vokrouhlický et al. 2006), a detailed discussion about the dependence of the simulations on this input parameter has been developed by de Elía & Brunini (2007). On the other hand, the exponent r_i in the mass-velocity model is given by

$$r_i = \frac{1-b_i}{k}, \quad (10)$$

(Petit & Farinella 1993; O'Brien & Greenberg 2005), where the value of k is about 9/4 (Gault et al. 1963). As for the constant coefficient C_i, it can be calculated from an energy conservation equation. Assuming that the relative kinetic energy $E_{\rm rel}$ of the collision is partitioned equally between the target and the projectile, so body i will receive an energy $E_i = E_{\rm rel}/2$ at impact. From this, we define $E_{{\rm fr},i} = f_{\rm ke}E_i$ as the kinetic energy of the fragments resulting from such body. $f_{\rm ke}$ is an inelasticity parameter determining which fraction of the energy received by a body is partitioned into kinetic energy of the fragments. In Sect. 4.4, we discuss some aspects of this parameter. On the other hand, while $E_{{\rm fr},i} = f_{\rm ke}E_i$, it can be also written following the mass-velocity model proposed. In fact,

$$E_{{\rm fr},i} = \lim_{\epsilon\to 0}\int_{\bar{M}_i}^{M_{{\rm max},i}-\epsilon}\frac{V^2}{2}mn_i(m){\rm d}m + \frac{V_{\rm max}^2}{2}M(\le\bar{M}_i) + \lambda_i\frac{V_{{\rm lf},i}^2}{2}M_{{\rm max},i}, \quad (11)$$

where $n_i(m){\rm d}m = -{\rm d}N_i(\ge m)$ and the last term is the kinetic energy of the largest fragment resulting from body i in a collision. The experimental studies performed by Fujiwara & Tsukamoto (1980) and Nakamura & Fujiwara (1991), indicate that the largest fragment resulting from a catastrophic fragmentation event has a negligible kinetic energy in the reference frame of the center of mass. On the other hand, in a cratering event, the largest fragment of mass $M_{{\rm max},i} = f_{l,i}M_{{\rm crat},i}$ (with $f_{l,i} = 0.2$) has a velocity $V_{{\rm lf},i}$ given by

$$V_{{\rm lf},i} = C_i M_{{\rm max},i}^{-r_i}. \quad (12)$$

So, in order to take into account this difference, we insert the corresponding term in the energy conservation equation multiplied by a factor λ_i, where λ_i will be 0 for a catastrophic event and 1 for a cratering event.

Equation (11) is an integral of m. Once V is written in terms of m (Eq. (9)), such integral can be evaluated. After solving for Eq. (11), the constant coefficient C_i will be given by the solution of the equation

$$aC_i^{k_i} + b - C_i^2 = 0, \quad (13)$$

where a and b are given by

$$\begin{aligned} a &= M_{{\rm max},i}^{2r_i+b_i-1}V_{\rm max}^{2-k_i}\left[\frac{2b_ir_i}{[(1-2r_i-b_i)\lambda_i + b_i](1-b_i)}\right] \\ b &= 2M_{{\rm max},i}^{2r_i-1}\left[\frac{1-b_i-2r_i}{(1-2r_i-b_i)\lambda_i + b_i}\right]E_{{\rm fr},i}, \end{aligned} \quad (14)$$

and $E_{{\rm fr},i}$ is assumed to be $f_{\rm ke}E_i$.

Once the fragment velocity distribution has been found for each of the bodies that participate in a collision, it is necessary to calculate the effective escape velocity $V_{\rm esc}$ from the gravitational field of the two colliding bodies. For this, we use the method developed by Petit & Farinella (1993) with the corrections made by O'Brien & Greenberg (2005). Thus, we calculate the escape velocity $V_{\rm esc}$ using the energy balance equation, which can be written as

$$\frac{1}{2}M^*V_{\rm esc}^2 + W_{\rm tot} = W_{{\rm fr},1} + W_{{\rm fr},2} + W_{\rm h}, \quad (15)$$

where $M^* = M_1 - M_{{\rm max},1} + M_2 - M_{{\rm max},2}$ if both bodies are catastrophically fragmented, $M^* = M_{{\rm crat},1} + M_2 - M_{{\rm max},2}$ if body 1 is cratered and body 2 is catastrophically fragmented and $M^* = M_{{\rm crat},1} + M_{{\rm crat},2}$ if both bodies are cratered. The term $W_{\rm tot}$ is the total gravitational potential energy of the two colliding bodies just before fragmentation event, which is given by

$$W_{\rm tot} = -\frac{3GM_1^{5/3}}{5Q} - \frac{3GM_2^{5/3}}{5Q} - \frac{GM_1M_2}{QM_1^{1/3} + QM_2^{1/3}}, \quad (16)$$

where the parameter Q is

$$Q = \left(\frac{4\pi\rho}{3}\right)^{-1/3}, \quad (17)$$

and ρ is the density of the objects. On the other hand, the terms $W_{\mathrm{fr},i}$ represent the gravitational potential energy of the fragments of body i resulting from the collision. If body i is catastrophically fragmented, $W_{\mathrm{fr},i}$ will be given by

$$W_{\mathrm{fr},i} = -\frac{3}{5}\frac{G}{Q}\int_{m=0}^{m=\infty} m^{5/3} n_i(m)\mathrm{d}m = -\frac{3G}{Q}\frac{M_{\mathrm{max},i}^{5/3}}{5-3b_i}, \quad (18)$$

while if body i is cratered, $W_{\mathrm{fr},i}$ will adopt the following expression

$$W_{\mathrm{fr},i} = -\frac{3}{5}\frac{G}{Q}\int_{m=0}^{m=\infty} m^{5/3} n_i(m)\mathrm{d}m - \frac{3G(M_i - M_{\mathrm{crat},i})^{5/3}}{5Q} = -\frac{3G}{Q}\frac{M_{\mathrm{max},i}^{5/3}}{5-3b_i} - \frac{3G(M_i - M_{\mathrm{crat},i})^{5/3}}{5Q}. \quad (19)$$

The term W_{h} is an estimate of the gravitational potential energy of the fragments when these are separated by a distance of the order of the Hill's radius of the total colliding mass in the gravitational field of the central mass M_{o} and orbital distance R_{o}. If both bodies are catastrophically fragmented, W_{h} is given by

$$W_{\mathrm{h}} = -\frac{3G(M_1 + M_2)^{5/3}}{5}\frac{(3M_{\mathrm{o}})^{1/3}}{R_{\mathrm{o}}}, \quad (20)$$

where M_{o} is the mass of the Sun and R_{o} is the orbital radius where the collision occurs. On the other hand, according to O'Brien & Greenberg (2005), if body 1 is cratered and body 2 is catastrophically fragmented, the term W_{h} must be written as

$$W_{\mathrm{h}} = -\frac{3G(M_2 + M_{\mathrm{crat},1})(M_1 - M_{\mathrm{crat},1})^{2/3}}{2}\frac{(3M_{\mathrm{o}})^{1/3}}{R_{\mathrm{o}}}, \quad (21)$$

while if both bodies are cratered, the term W_{h} has the form

$$W_{\mathrm{h}} = -3G(M_1 + M_2 - M_{\mathrm{crat},1} - M_{\mathrm{crat},2})^{2/3} \times \frac{(M_{\mathrm{crat},1} + M_{\mathrm{crat},2})}{2}\frac{(3M_{\mathrm{o}})^{1/3}}{R_{\mathrm{o}}}. \quad (22)$$

Once the different W terms are calculated, it is possible to find the escape velocity V_{esc} from the corresponding energy balance equation. From this, in Sect. 4.5 we describe the treatment proposed in our algorithm in order to study the escape and reaccumulation processes of the ejected fragments.

3. Dynamical features

The Trojan asteroids are locked in a 1:1 mean motion resonance with Jupiter librating around the Lagrangian equilibrium points L_4 and L_5. Figure 1 shows the distribution of 1155 Jovian Trojans associated to the L_4 swarm, with respect to semimajor axis a, eccentricity e and inclination i. Such plots indicate that all Jupiter Trojans observed in L_4 present a, e and i values ranging between 4.7 and 5.7 AU, 0 and 0.3, and 0 and 60°, respectively. In the following, these will be the boundaries of L_4 in semimajor axis, eccentricity and inclination with which we are going to perform our work. Assuming that the positions occupied by the asteroids in the planes ae and ai represent stable zones of the swarm, it is possible to define a set of stability and instability niches within of the boundaries of the cloud. In fact, we construct such regions assuming widths of 0.02 AU, 0.0125 and 2.25° in semimajor axis, eccentricity and inclination, respectively. The

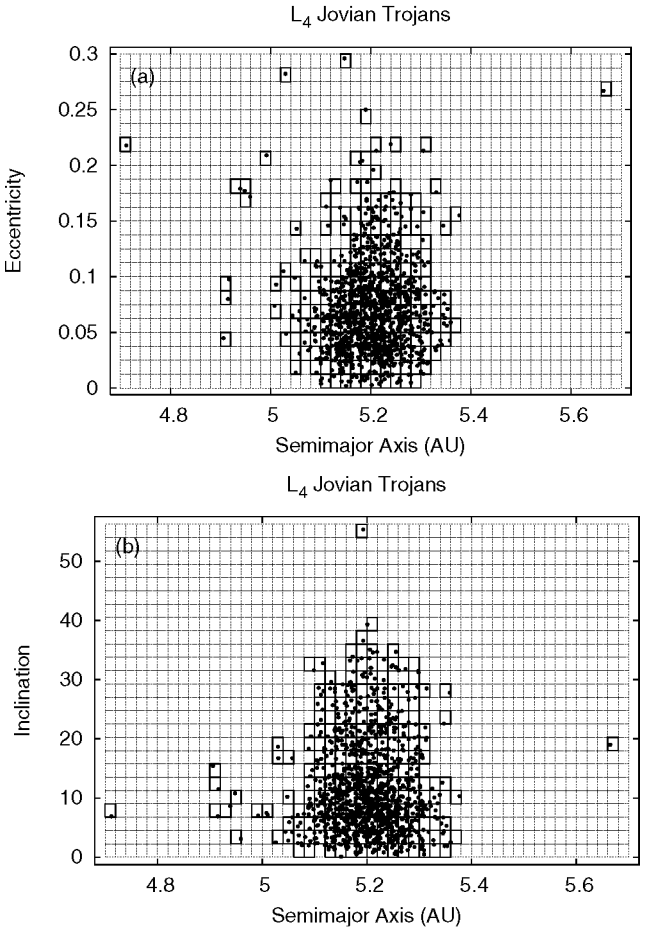

Fig. 1. The distribution of the population of L_4 with respect to semimajor axis, eccentricity and inclination. The solid and dashed squares represent the stability and instability niches used in our simulations, respectively. (Data obtained from `http://www.cfa.harvard.edu/iau/lists/JupiterTrojans.html`)

stability and instability niches generated from this procedure are indicated in Fig. 1 as solid and dashed squares, respectively.

Another important question concerning the dynamical behavior of the Trojan asteroids is their libration amplitude distribution. From Marzari et al. (2002), the libration amplitudes ranging from 0.6° to 88.7°, with a mean value of 32.7° for the L_4 cloud. A detailed discussion about the distribution of the libration amplitude of the Trojan asteroids can be found in Marzari et al. (2003).

Section 4.5 describes how the stability and instability niches shown in Fig. 1 are included in our numerical algorithm in order to model the dynamical treatment of the code, as well as how the mean libration amplitude is used to determine the final fate of the Trojan fragments. On the other hand, we discuss in Sect. 5.4 the sensitivity of our results to the way those niches were constructed as well the dependence of our simulations on the initial orbital element distribution of the population.

4. Collisional and dynamical evolution model

In this section, we present the full model we use to study the collisional and dynamical evolution of the population of L_4 Jovian Trojans.

4.1. Population of the model

The population and size distribution of the Trojan asteroids was studied by Jewitt et al. (2000) who developed an optical survey in the direction of the L_4 swarm. According to this work, the differential size distributions of the L_4 Trojans are given by

$$n_1(r_{0.04})\mathrm{d}r_{0.04} = 1.5\times 10^6\left(\frac{1\ \mathrm{km}}{r_{0.04}}\right)^{3.0\pm0.3}\mathrm{d}r_{0.04} \quad (23)$$

for $2.2 \le r_{0.04} \le 20$ km, and

$$n_2(r_{0.04})\mathrm{d}r_{0.04} = 3.5\times 10^9\left(\frac{1\ \mathrm{km}}{r_{0.04}}\right)^{5.5\pm0.9}\mathrm{d}r_{0.04} \quad (24)$$

for $r_{0.04} \ge 42$ km, while the corresponding integral distributions are

$$N(>r_{0.04}) = 1.6\times 10^5\left(\frac{1\ \mathrm{km}}{r_{0.04}}\right)^{2.0\pm0.3} \quad (25)$$

for $2.2 \le r_{0.04} \le 20$ km, and

$$N(>r_{0.04}) = 7.8\times 10^8\left(\frac{1\ \mathrm{km}}{r_{0.04}}\right)^{4.5\pm0.9} \quad (26)$$

for $r_{0.04} \ge 42$ km, where $r_{0.04}$ is the radius derived assuming a geometric albedo of 0.04, which is the mean value of known Trojans (Tedesco 1989).

Some years later, Yoshida & Nakamura (2005) analyzed the size distribution of faint Jovian L_4 Trojan asteroids corresponding to the radius range of $1 \le r_{0.04} \le 5$ km. For this entire range, these authors derived a value for the mean slope of the cumulative size distribution of 1.9 ± 0.1, which is consistent with that previously estimated by Jewitt et al. (2000) for the L_4 Trojans with $2.2 \le r_{0.04} \le 20$ km (see Eq. (25)). However, Yoshida & Nakamura (2005) noted that the size distribution of detected L_4 Trojans shows a slight break at $r_{0.04} \sim 2.5$ km by deriving mean slopes of the cumulative size distribution of 1.28 ± 0.11 for $1 \le r_{0.04} \le 2.5$ km and 2.39 ± 0.10 for $2.5 \le r_{0.04} \le 5$ km.

The numerical simulations performed by Davis & Weidenschilling (1981) and Marzari et al. (1997) indicate that the larger Trojan asteroids would be unaltered by catastrophic impacts since the early stages of the Solar System history. Binzel & Sauter (1992) reported lightcurve observations for Trojan asteroids indicating that only those with $r_{0.04} > 45$ km have been able to retain their initial forms after 4.5 Gyr of collisional evolution. From this, these authors suggested that a 45 km radius may represent a transition between a primordial population and collisional fragments produced from larger bodies. On the other hand, Jewitt et al. (2000) found a critical radius of approximately 30 km for the L_4 Trojan size distribution, which can be seen by equating Eqs. (25) and (26). Jewitt et al. (2000) concluded that since the transition radius estimated by Binzel & Sauter (1992) is uncertain to within a factor of 2, the size distribution as well as the lightcurve amplitude distribution of Trojan asteroids indicate that a primordial/fragment transition occurs at a radius near 30–40 km. Thus, for $r > 30$ km, we construct an initial population that follows an cumulative power-law index with a value close to the observed slope of Trojans in this size range (see Eq. (26)), while for $r \le 30$ km, we assign an cumulative power-law index p in order to reproduce a given initial mass. From this, the cumulative starting population used in our model to study the L_4 swarm is defined as follow

$$N(>r) = C\left(\frac{1\ \mathrm{km}}{r}\right)^p \quad \text{for} \quad r \le 30\ \mathrm{km},$$
$$N(>r) = 2.3\times 10^9\left(\frac{1\ \mathrm{km}}{r}\right)^{4.7} \quad \text{for} \quad r > 30\ \mathrm{km}, \quad (27)$$

where $C = 2.3\times 10^9\ (30)^{-4.7}\ (30)^p$ by continuity for $r = 30$ km. In our simulations, p is assumed to be 3 which leads to an initial population of ~8 times the current L_4 Trojan swarm mass, which is of order 5×10^{23} g (Jewitt et al. 2000). It represents a collisionally evolved population whose members could have been captured as Trojans after a significant amount of small bodies had been generated from collisions between planetesimals orbiting near Jupiter (Marzari et al. 1997). Figure 2 shows the starting cumulative size distribution used in our simulations together with the integral distribution derived by Jewitt et al. (2000).

In Sect. 5.4, we discuss the dependence of our simulations on the initial population.

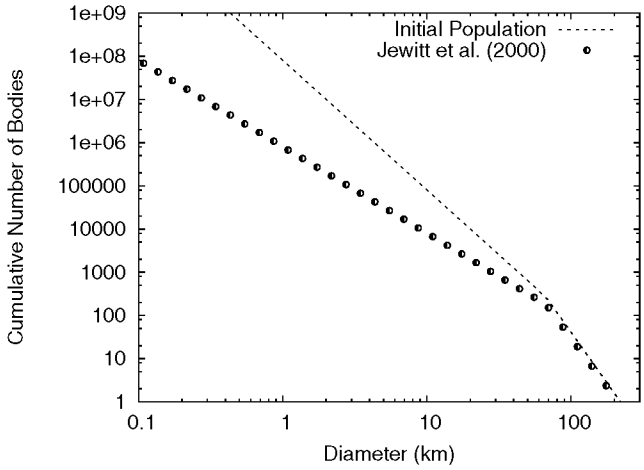

Fig. 2. Initial population of the model. The black points show the integral distribution derived by Jewitt et al. (2000) for the L_4 Trojan asteroids.

4.2. Collision velocities and probabilities

Mean values for the intrinsic collision probability $\langle Pi_c\rangle$, which describes how frequently collisions occur, and the impact velocity $\langle V\rangle$ are fundamental quantities for any collisional evolution study. We adopt the values of $\langle Pi_c\rangle$ and $\langle V\rangle$ derived by Dell'Oro et al. (1998) using the mathematical algorithm developed by Dell'Oro & Paolicchi (1998) on a sample of 223 Trojans. This statistical method computes the values of $\langle Pi_c\rangle$ and $\langle V\rangle$ for the two Trojan swarms over a long timescale of 1 Myr, taking into account the dynamical links among the Trojans and Jupiter orbital angles due to the 1:1 resonance. Over a long timescale the effect of the secular frequency $g_5 - g_6$ becomes important, strongly affecting the semimajor axis, the eccentricity and the libration amplitude of all Trojan asteroids. For that reason, the $\langle Pi_c\rangle$ time evolution shows large oscillations around the average value while the behavior of $\langle V\rangle$ is somewhat more complicated due to the variations in inclination of Trojans. The mean values of the impact velocity and the intrinsic collision probability derived by Dell'Oro et al. (1998) for the two Trojan asteroid swarms are shown in Table 1.

Table 1. Mean values for the impact velocity $\langle V \rangle$ and the intrinsic collision probability $\langle Pi_c \rangle$ derived by Dell'Oro et al. (1998) for the two Trojan asteroid swarms, from a sample of 223 objects.

	$\langle Pi_c \rangle$ $\times 10^{-18}$ km^{-2} yr^{-1}	$\langle V \rangle$ km s^{-1}
L_4	7.79 ± 0.67	4.66
L_5	6.68 ± 0.18	4.51

4.3. Interrelations with Hildas and Jupiter-family comets

Apart from mutual collisions, Trojan asteroids can also have encounters with Hilda asteroids and Jupiter-family comets. To understand if such populations contribute to the collisional evolution of Trojans, it is necessary to analyze the following two important points:

- the intrinsic collision probabilities $\langle Pi_c \rangle$, between Trojans and Hildas and between Trojans and Jupiter-family comets;
- the estimated total number of Hilda asteroids and Jupiter-family comets able to impact the population of Trojans.

Dahlgren (1998) and Dell'Oro et al. (2001) estimated the intrinsic collision probability $\langle Pi_c \rangle_{T-H}$ between Trojans and Hildas and found that the value of $\langle Pi_c \rangle_{T-H}$ is around a factor of 30 lower than $\langle Pi_c \rangle_{T-T}$ for collisions between L_4 Trojan asteroids. In addition, Brunini et al. (2003) determined that the total number of Hildas with radius larger than 1 km is at most 25 000, which is approximately 16% of the estimated population at the L_4 Trojan swarm by Jewitt et al. (2000), of 1.6×10^5 asteroids (see Eq. (25)). In the same way, Dell'Oro et al. (2001) computed the intrinsic collision probability $\langle Pi_c \rangle_{T-JFC}$ between L_4 Trojans and Jupiter-family comets and determined that the value of $\langle Pi_c \rangle_{T-JFC}$ is almost a factor 24 lower than $\langle Pi_c \rangle_{T-T}$ for collisions between L_4 Trojan asteroids. Moreover, Fernández et al. (1999) indicated that the total number of Jupiter-family comets larger than 0.7 km in radius is estimated to be from several thousands to about 10^4, which is from one to two orders of magnitude smaller than the total number of L_4 Trojans derived by Jewitt et al. (2000) (see Eq. (25)).

From this, we infer that the contribution of Hilda asteroids and Jupiter-family comets to the collisional evolution of Trojan asteroids is negligible.

4.4. Asteroid strength

O'Brien & Greenberg (2005) showed that the general shape of the final evolved asteroid population is determined primarily by Q_D, but variations in Q_S and f_{ke} can affect such final population even if Q_D is held the same. According to these arguments we choose Q_S and f_{ke} as input parameters of our collisional model. In fact, we test different Q_S laws and use a parameter f_{ke} depending on target size (Davis et al. 1995; O'Brien & Greenberg 2005) which are combined to yield the Q_D law derived by Benz & Asphaug (1999) from hydrodynamic studies for icy bodies at 3 km s^{-1}. Such Q_D law is shown in Fig. 3 as a solid line and can be calculated from an expression of the form

$$Q_D = C_1 D^{-\lambda_1}(1 + (C_2 D)^{\lambda_2}), \tag{28}$$

where C_1, C_2, λ_1, and λ_2 are constant coefficients whose values are 24, 2.3, 0.39 and 1.65, respectively.

To analyze the dependence of our numerical simulations on the shattering impact specific energy Q_S, we use a numerous family of Q_S curves testing different slopes in the "gravity-scaled regime" and covering all the possibilities from small to large gaps between Q_S and the Q_D law from Benz & Asphaug (1999). In fact, the Q_S laws used in our simulations are shown in Fig. 3 as dashed lines and can be also represented from expressions of the form

$$Q_S = C_1 D^{-\lambda_1}(1 + (C_2 D)^{\lambda_2}), \tag{29}$$

where C_1, C_2, λ_1, and λ_2 are constant coefficients. For small bodies, with diameters $\lesssim$1 km, the gravitational binding energy is negligible and owing to that Q_S and Q_D have the same value. Thus, the values of C_1 and λ_1 for all the Q_S laws must be equal to those specified for the Q_D law from Benz & Asphaug (1999) since such coefficients dominate the behavior of the curves for small sizes. On the other hand, the coefficients λ_2 and C_2 determine the slope and the magnitude of every Q_S law in the "gravity-scaled regime", respectively. The values of λ_2 used in Figs. 3a–d are 2, 1.75, 1.5 and 1.25, respectively. As for C_2, this coefficient ranges from 0.5 to 0.15, from 1.2 to 0.2, from 2 to 0.8 and from 2.3 to 1 for the Q_S laws shown in Figs. 3a–d, respectively.

On the other hand, f_{ke} is a poorly known parameter in collisional processes. But, many authors have suggested that it may vary with size, with impact speed and probably with the material properties. Thus, according to that made by O'Brien & Greenberg (2005), we express the parameter f_{ke} as

$$f_{ke} = f_{ke_0}\left(\frac{D}{1000\ \text{km}}\right)^{\gamma}. \tag{30}$$

The values of f_{ke_0} and γ used in our simulations are 0.35 and 0.7, respectively. Such values are according to that discussed by O'Brien & Greenberg (2005), who indicate that γ is on the order of 0.5 (always between 0 and 1) and f_{ke_0}, the value at 1000 km, is ~0.05–0.3, which is consistent with estimates of f_{ke} in large impacts (Davis et al. 1989). An interesting result is that the values of f_{ke_0} and γ do not depend on the Q_S law to yield a given Q_D. In fact, from the combination of any of the Q_S laws shown in Fig. 3 and f_{ke}, with $f_{ke_0} = 0.35$ and $\gamma = 0.7$, the Q_D law derived by Benz & Asphaug (1999) is obtained with good accuracy.

4.5. The full model

In order to simulate the collisional and dynamical evolution of the Jovian Trojan asteroids of the L_4 swarm, our numerical code evolves in time the number of bodies residing in a set of 130 discrete logarithmic size bins, whose central values range from $D_1 = 10^{-10}$ km to $D_{130} = 886.7$ km in diameter in such a way that from one bin to the next, the mass of the bodies changes by a factor of 2 and the diameter changes by a factor of $2^{1/3}$, adopting a density of 1.5 g cm^{-3}.

Following Campo Bagatin et al. (1994) and Campo Bagatin (1998), a collisional system with a low-mass cutoff leads to waves in the size distribution of the bodies. In order to avoid this effect, we do not evolve in time the 60 first size bins, whose central values range from 10^{-10} to 10^{-4} km. In fact, this part of the population is only used as a tail of projectiles for calculating impact rates with larger bodies and its size distribution is determined each timestep by extrapolating the slope of the distribution of the ten next size bins.

In each timestep, a characteristic orbit is generated at random for each collision between Trojans of diameters D_1 and D_2 in the L_4 swarm. For this, we use the acceptance-rejection method developed by John von Neumann. From Figs. 1a and 1b, we construct 3-D niches within of the boundaries of L_4 with widths of 0.02 AU, 0.0125 and 2.25° in semimajor axis a, eccentricity e

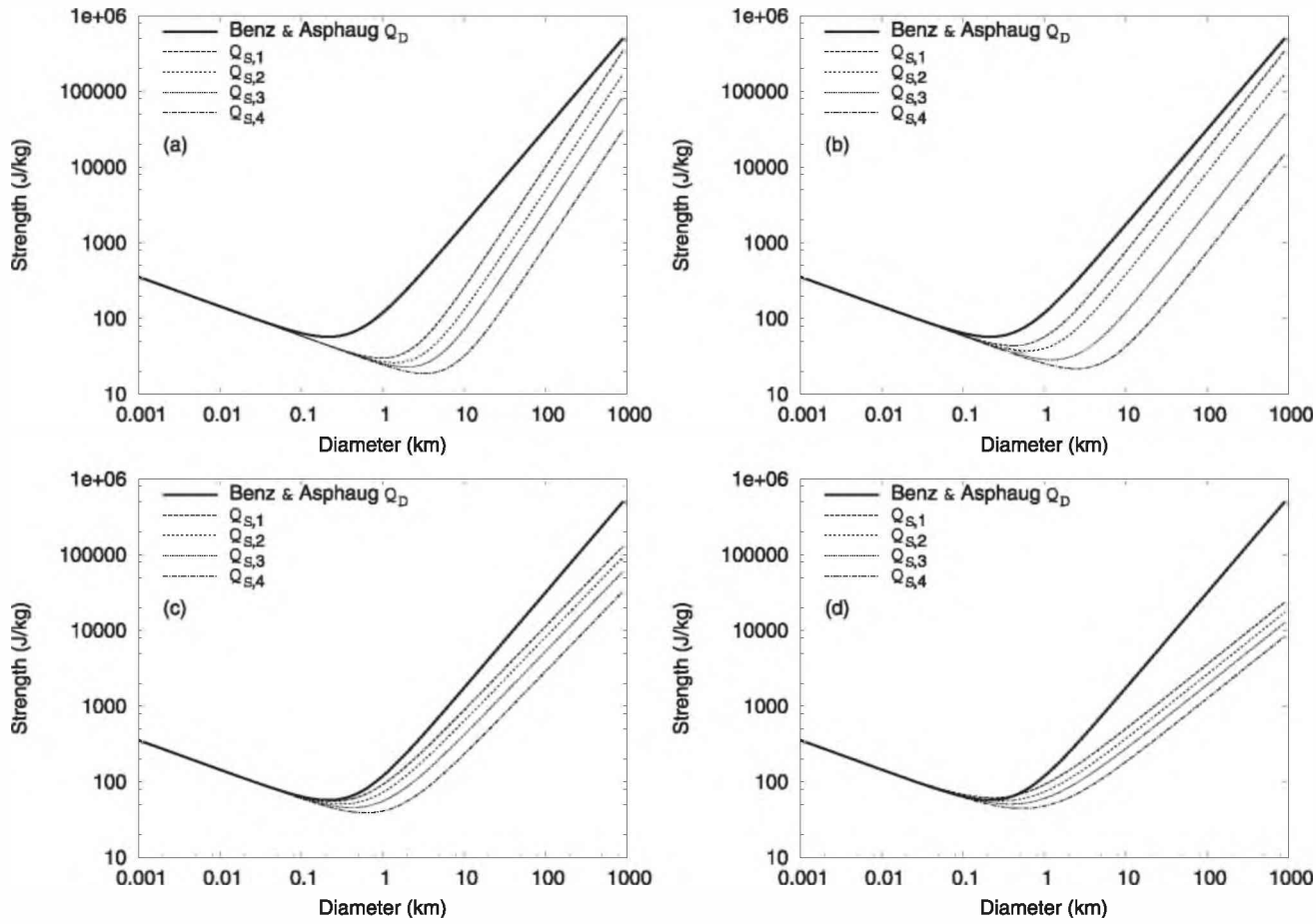

Fig. 3. Asteroid strength. The dashed lines represent the Q_S laws used in our simulations. From **a)** to **d)**, the Q_S curves show decreasing slopes in the "gravity-scaled regime" covering all the possibilities from small to large gaps between Q_S and the Q_D law from Benz & Asphaug (1999) for icy bodies at 3 km s^{-1}, which is plotted as a solid line.

and inclination i, respectively. In each of these zones, we calculate the fraction of Trojan asteroids $f(a,e,i) = N^{\text{Trojan}}_{(a,e,i)}/N^{\text{Trojan}}_{\text{Total}}$, where $N^{\text{Trojan}}_{\text{Total}}$ represents the total number of Trojans of the sample, which is equal to 1155 (see Sect. 3). This procedure allows us to define a function f of a, e and i whose maximum value results to be of ~0.0065. The acceptance-rejection technique of von Neumann indicates that if a set of numbers a^*, e^* and i^* is selected randomly from the domain of the function f (namely, a^*, e^* and i^* between 4.7 and 5.7 AU, 0 and 0.3 and 0 and 60°, respectively), and another set of numbers f^* is given at random from the range of such function (namely, f^* between 0 and 0.0065), so the condition $f^* \leq f(a^*, e^*, i^*)$ will generate a distribution for (a^*, e^*, i^*) whose density is $f(a^*, e^*, i^*)\mathrm{d}a^*\mathrm{d}e^*\mathrm{d}i^*$. Such (a^*, e^*, i^*) values will be accepted as possible initial conditions for the semimajor axis, eccentricity and inclination of the L_4 Trojans, in agreement with the observational data. It is worth noting that in mean motion resonances, the evolution of a, e and i is coupled. However, we are treating them as uncorrelated variables. Nevertheless, a more rigorous treatment would be very difficult, and we believe the results would be not too different than the ones found here. Finally, given the longitude of ascending node Ω, the argument of pericentre ω and the mean anomaly M between 0 and 360°, an orbit can be assigned and from this, a position-velocity pair can be derived for every of the colliding Trojans.

Once a typical orbit has been computed for each body participating of a given collision, the next step is to carry out the collisional treatment (including the analysis of the reaccumulation process) from the algorithm outlined in Sect. 2. In order to determine the final fate of the fragments escaping from the gravitational field of the system, it is necessary to calculate which are their orbital elements once they are ejected with a relative velocity with respect to the parent body. Immediately before the collision, the barycentric position and velocity of the fragments are assumed to be those associated with their parent body. After the collision, we consider that the barycentric position of the fragments does not change while the relative velocities with respect to their parent body (Eq. (9)) are assumed to be equally partitioned between the three components. Once the barycentric position and velocity of the fragments after the collision have been obtained, it is possible to calculate their orbital elements and the final fate of them. For this, we use the following criterion:

1. The fragments remain in the L_4 Jovian swarm if the combinations of (a, e) and (a, i) values are associated with some of the stability niches shown in Figs. 1a and 1b, respectively, and the absolute value of the difference between their final and initial mean longitudes is smaller than the mean libration amplitude for the L_4 Trojan asteroids, which is assumed to be ~30° in agreement with that discussed in Sect. 3. The mean longitude is denoted by λ and is defined by

$$\lambda = M + \Omega + \omega, \tag{31}$$

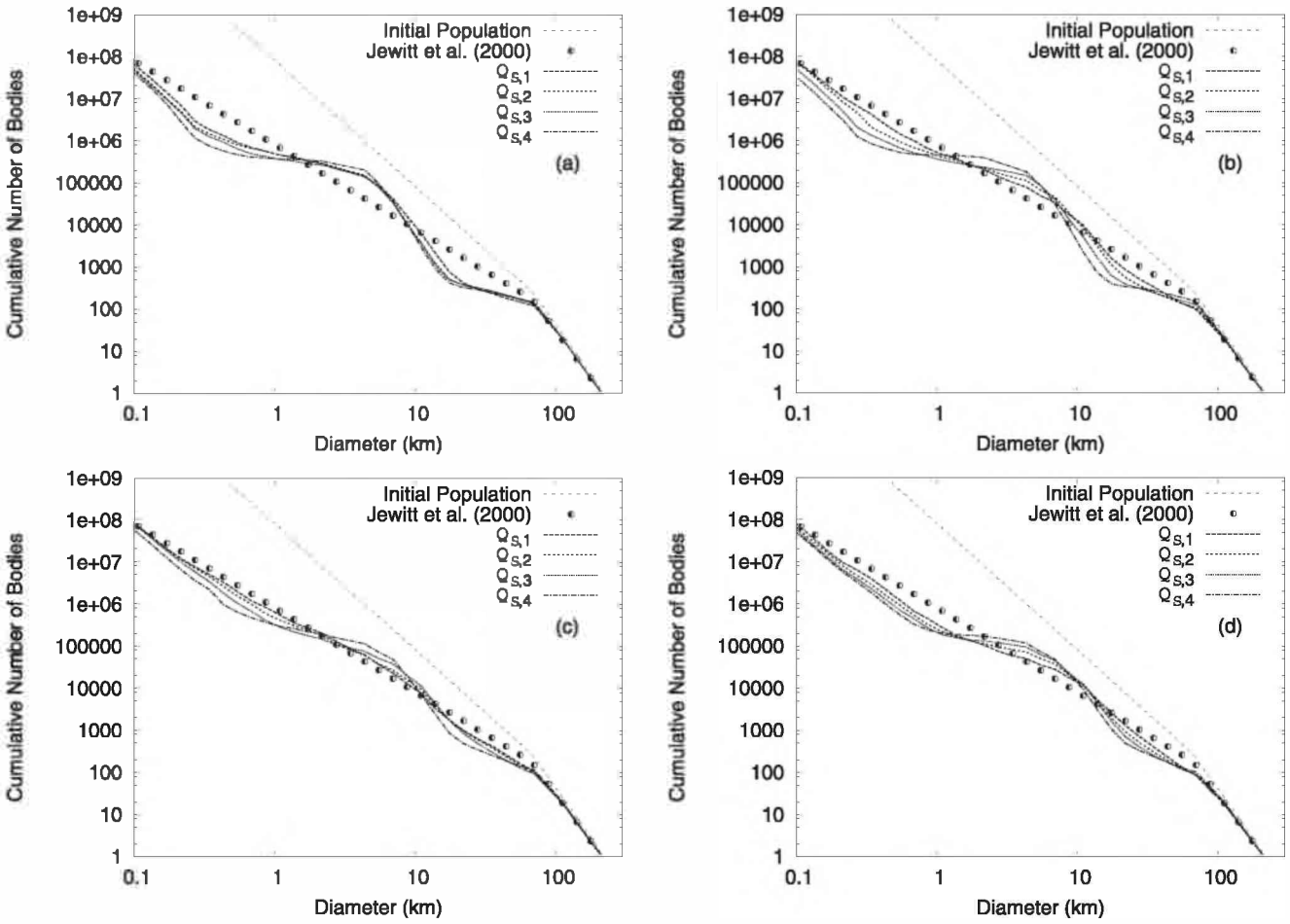

Fig. 4. Our estimates of the L_4 Trojan cumulative size distribution obtained from the Q_S laws presented in Figs. 3a–d are shown in **a)–d)**, respectively. Data derived by Jewitt et al. (2000) from optical surveys are given for comparison.

where M, Ω and ω represent the mean anomaly, the longitude of ascending node and the argument of pericentre, respectively.

2. On the other hand, the fragments are ejected from the L_4 Jovian swarm no longer participating in the collisional evolution if any of the following conditions is fulfilled:
   - eccentricity $e \geq 1$;
   - (a, e, i) values exceed the boundaries of the L_4 swarm (see Sect. 3);
   - (a, e) and (a, i) values are associated with some of the instability niches shown in Figs. 1a and 1b, respectively;
   - (a, e) and (a, i) values are associated with some of the stability niches shown in Figs. 1a and 1b, respectively; but the absolute value of the difference between the initial and final mean longitudes is larger than the mean libration amplitude of ~30°.

To study the evolution in time of the L_4 Trojan population, the timestep Δt is calculated in such a way that the change of the number of objects in any size bin is always smaller than a given amount, which is generally chosen as 1% of the original number of bodies.

5. Results

We have developed a series of numerical simulations aimed at studying the collisional and dynamical evolution of the L_4 Trojan asteroids for different Q_S laws which cover all the possibilities from small to large gaps between Q_S and the Q_D law derived by Benz & Asphaug (1999) for icy bodies at 3 km s^{-1}. Here, we discuss the general outcomes obtained from the numerous family of Q_S curves presented in Sect. 4.4. Thus, in Sect. 5.1, we compare our estimates of the L_4 Trojan cumulative size distribution to that derived by Jewitt et al. (2000) from optical surveys. Moreover, we present results concerning the mean collisional lifetimes of Trojans. In Sect. 5.2, we compare the number of large asteroid families obtained from our work to those studied by Beaugé & Roig (2001), Dotto et al. (2006) and Fornasier et al. (2007). Then, in Sect. 5.3, we analyze our results in regard to the ejection rates of Trojan fragments, investigating their possible contribution to the population of Centaurs and Jupiter-family comets. Finally, we study in Sect. 5.4 the dependence of our results on the dynamical model, the initial mass of the Trojan population and the initial distribution of orbital elements.

5.1. L_4 Trojan cumulative size distributions

Figures 4a–d show our estimates of the L_4 Trojan cumulative size distribution obtained from the family of Q_S curves presented in Figs. 3a–d, respectively. The results of our simulations show waves that propagate from diameters of ~0.1 to ~80 km around of the values derived by Jewitt et al. (2000) from optical surveys. From O'Brien & Greenberg (2003), waves form in the population as a result of a change in impact strength properties

at a given diameter, which was previously discussed in Sect. 2.1 and can be observed in the Q_S and Q_D laws presented in Fig. 3. In fact, O'Brien & Greenberg (2003) indicated that if all bodies were in the gravity-scaled regime, the resulting evolved population would follow the general trend of a power law without to produce a wavy structure. According to these authors, the transition from a strength to a gravity-scaled regime at a given diameter D_t leads to an overabundance of impactors capable of destroying bodies of such diameter compared to that what would be expected if all bodies had a gravity-scaled impact specific energy. This generates a larger decrease in objects of diameter D_t which produces an overabundance of bodies that can be destroyed by projectiles of such size, leading to a decrease in larger bodies and so on. From this, a wave forms in the population since the transition diameter D_t and then propagates to larger sizes.

For all our numerical experiments, the positions of the peaks and valleys of the wave do not significantly change. In fact, Figs. 4a–d show that the first valley extends from diameters of ~0.1 to 1 km producing a peak around of 5 km, which leads to a second valley at a diameter of about 20 km. These results allow us to infer that the general shape of the final evolved population is determined primarily by the dispersing impact specific energy Q_D rather than by shattering impact specific energy Q_S, which is consistent with that discussed by O'Brien & Greenberg (2005). On the other hand, the break at $D \sim 5$ km found here is in agreement with that discussed by Yoshida & Nakamura (2005).

However, an interesting result obtained from our study is that the largest gaps between Q_S and Q_D curves lead to the largest wave amplitudes. In order to understand this behavior, we carry out two numerical simulations aimed at analyzing how the dispersion process of fragments resulting from catastrophic and cratering events is affected by the relation between Q_S and Q_D. To do it, we select the $Q_{S,1}$ and $Q_{S,4}$ laws presented in Fig. 3b, which show a small and a large gap with the Q_D law from Benz & Asphaug (1999), respectively. The simulation using the specified $Q_{S,4}$ law shows that the number of dispersed fragments with diameters larger than 0.1 km resulting from catastrophic and cratering events is ~55–75% less compared to that derived from the simulation with the smaller gap (see Fig. 5a). Moreover, more than 99 percent of the total of dispersed fragments larger than 0.1 km in diameter lies in the first valley of the wave (namely, in the ~0.1 to 1 km diameter range) for both numerical simulations. In fact, the number of dispersed fragments with $D \geq 1$ km results to be some orders of magnitude smaller than the total number of dispersed fragments with $D \geq 0.1$ km (see Figs. 5a and b). Thus, the number of fragments capable of replenishing size bins in the 0.1 to 1 km diameter range is significantly smaller for the simulation that uses the larger gap between Q_S and Q_D. This result implies that the first valley of the wave is deeper for larger gaps between Q_S and Q_D, leading to a larger amplitude for the following peak and so on. This analysis allows us to understand why the larger the gap, the larger the wave amplitude.

On the other hand, the general outcomes indicate that the mean collisional lifetimes of Trojan asteroids in the gravity-scaled regime obtained from numerical simulations with a large gap between Q_S and Q_D laws, are smaller than those derived from simulations with a small gap. Figure 6 allows us to see this behavior, showing representative results concerning the mean collisional lifetimes of Trojans with $D \geq 0.1$ km, using the $Q_{S,1}$ and $Q_{S,4}$ laws from Fig. 3b, which have a small and a large gap with the Q_D law from Benz & Asphaug (1999), respectively. In fact, according to that discussed in Sect. 2.1 and Eqs. (1) and (2),

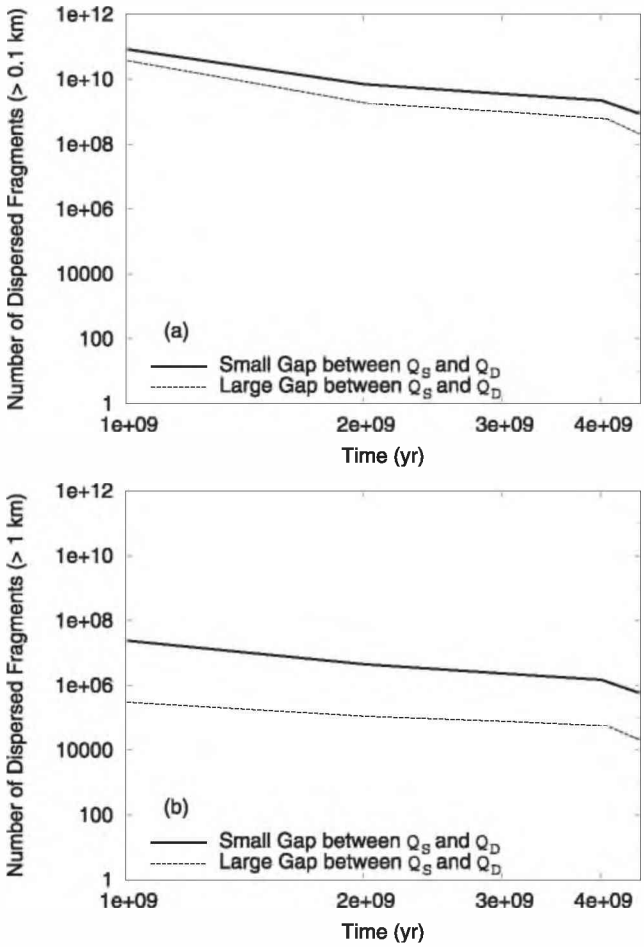

Fig. 5. Number of dispersed bodies with $D \geq 0.1$ km **a)** and 1 km **b)** resulting from catastrophic impacts and cratering events as a function of time. These results have been obtained from the $Q_{S,1}$ and $Q_{S,4}$ laws presented in Fig. 3b, which show a small and a large gap with the Q_D law from Benz & Asphaug (1999), respectively.

the diameter D_p of the smaller projectile capable of catastrophically fragment a target with diameter D can be approximated by

$$D_p = \left(\frac{4Q_S}{V^2}\right)^{1/3} D, \tag{32}$$

where V is the relative impact velocity and Q_S is the shattering impact specific energy of target. For a large gap between Q_S and Q_D laws, Q_S values for objects in the gravity-scaled regime are smaller than those associated to a small gap. Thus, the larger the gap, the smaller the D_p values for targets with $D \geq 0.1$ km. Then, in general terms, numerical simulations with a large gap have more projectiles capable of shattering a given target belonging to the gravity-scaled regime than simulations with a small gap. On the other hand, Fig. 6 shows that the large Trojans have mean lifetimes longer than the age of the Solar System, which implies that such asteroids have likely survived unaltered by catastrophic impacts over the Solar System history, in agreement with that discussed by Davis & Weidenschilling (1981) and Marzari et al. (1997).

5.2. Trojan families

The existence of asteroid families in the L_4 Jovian swarm represents a clear consequence of the collisional activity in this

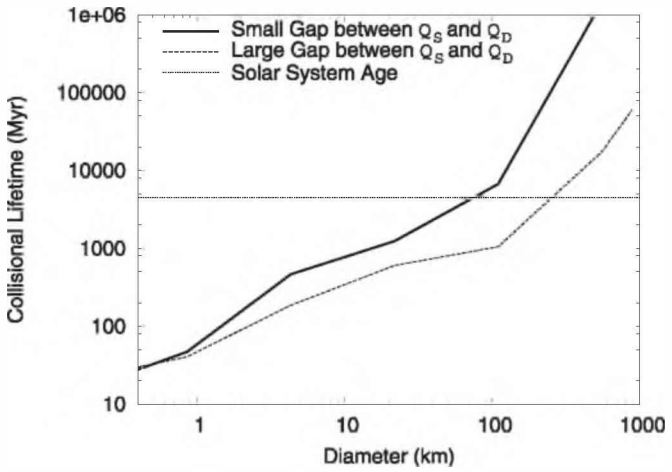

Fig. 6. Mean collisional lifetimes of L_4 Trojans obtained using the $Q_{S,1}$ (solid line) and $Q_{S,4}$ (large-dashed line) laws presented in Fig. 3b, which show a small and a large gap between Q_S and the Q_D law from Benz & Asphaug (1999), respectively. The horizontal short-dashed line represents the age of the Solar System.

population. In the early 2000s, Beaugé & Roig (2001) developed a semi-analytical model for the motion of the Trojan asteroids. From this algorithm, accurate proper elements were estimated for a set of 533 Trojans, which allowed to identify the existence of two robust asteroid families around L_4, known as Menelaus and Epeios. Menelaus is the most reliable candidate to be a real family whose members present a size distribution with only two asteroids of ~80 km in diameter, three objects in the 40–50 km range, plus a large number of small bodies with sizes of the order of 20–30 km. On the other hand, the size distribution of the family of Epeios is very different to that of Menelaus since all its members present diameters less than 40 km. Some years later, Dotto et al. (2006) made use of the list of Jupiter Trojan families provided by Beaugé & Roig (2001) and studied the surface properties of several members belonging to the Menelaus, 1986 WD and Makhaon L_4 families from a visible and near-infrared spectroscopic and photometric survey of Jovian Trojans. Then, in the framework of the same project, Fornasier et al. (2007) analyzed the main characteristics of small and large members associated to the Eurybates, Menelaus, 1986 WD and 1986 TS6 families in the L_4 swarm. These surveys indicate that all Eurybates family members, except the largest member whose diameter is ~70 km, are smaller than ~40 km. On the other hand, the members of the 1986 WD present a size distribution with a few objects larger than ~50 km in diameter, plus some bodies with sizes smaller than 40 km. Moreover, all members of the Makhaon and 1986 TS6 families present diameters smaller than ~55 km.

Given the size distributions of members of the L_4 families studied by Beaugé & Roig (2001), Dotto et al. (2006) and Fornasier et al. (2007), we analyze the formation of Trojan families from the breakup of parent bodies with diameters larger than 50 and 100 km that disperse fragments smaller than ~40 km. Simulations with the largest gaps between Q_S and Q_D do not form any of such families, which rules out those Q_S laws as possible shattering impact specific energies for the L_4 Trojan asteroids. On the other hand, simulations with the smallest gaps between Q_S and Q_D, except that using the $Q_{S,1}$ law from Fig. 3b, lead to the formation of 2 Trojan families from the breakup of parent bodies larger than 100 km in diameter, but do not produce families from objects in the 50 to 100 km diameter range. Our results predict that the first of such families is formed about 3.5 Gyr ago while the second one is generated during the last hundred Myr of evolution. For the $Q_{S,1}$ law from Fig. 3b, 9 Trojan families are formed by the breakup of bodies with diameters larger than 100 km, while 5 big bodies in the 50 to 100 km diameter range are collisionally disrupted over 4.5 Gyr. According to this simulation, the formation of such families starts since the first few Myr of collisional evolution and remains over the Solar System age. These results are in agreement with the number of L_4 Trojan families studied by Beaugé & Roig (2001), Dotto et al. (2006) and Fornasier et al. (2007), suggesting moreover that new families should be identified in the future.

5.3. Ejection rates

Figures 7a–d show the number of bodies ejected from the L_4 Jovian swarm with diameters larger than 1 km per Myr as a function of time over the age of the Solar System, obtained from the Q_S laws presented in Figs. 3a–d, respectively. In general terms, the largest gaps between Q_S and Q_D lead to the smallest ejection rates of Trojans from the L_4 swarm. To understand this behavior, we analyze the results concerning the dispersion of fragments obtained from the two numerical simulations carried out in Sect. 5.1, selecting the $Q_{S,1}$ and $Q_{S,4}$ laws from Fig. 3b, which show a small and a large gap with the Q_D law from Benz & Asphaug (1999), respectively. Our study allows us to infer that, for the larger gap between Q_S and Q_D laws, the number of dispersed fragments with diameters larger than 1 km resulting from catastrophic and cratering events is ~95% less than that obtained from the numerical experiment that uses the smaller gap (see Fig. 5b). This indicates that the simulation with the larger gap between Q_S and Q_D produces a significantly smaller number of fragments of $D \gtrsim 1$ km that can be ejected from the L_4 swarm compared to that derived with the smaller gap. This allows us to understand the general trend of our results concerning the ejection rates of Trojans from the L_4 cloud.

In Sect. 4.5, we discussed several criterions to determine the final fate of the Trojan fragments and from this to calculate the ejection rates from the L_4 Jovian swarm. From all our numerical experiments, we find that fragments escaping from L_4 present eccentricities $e < 1$ (see Fig. 8a), which rules out the parabolic or hyperbolic collisional ejection as a Trojan removal source. On the other hand, when an impact occurs, the absolute value of the difference between the initial and final mean longitudes of the colliding Trojans is always smaller than the mean libration amplitude of ~30°, which indicates that the collisions in the L_4 Trojan swarm do not allow the ejection of fragments from relevant changes in the librational behavior. For all our simulations, the ejection of Trojan fragments from L_4 is due to variations in the a, e and i values, which associate to some instability niches shown in Fig. 1 or exceed the boundaries of the swarm (see Sect. 3). Figure 8 shows a representative sample of the distribution of Trojans ejected from L_4 with respect to semimajor axis, eccentricity and inclination.

On the other hand, for all cases, most of the bodies ejected from the L_4 swarm with diameters larger than 1 km have diameters ranging from 1 to 5 km. In fact, our simulations show that the number of fragments of $D > 5$ km removed per unit time from L_4 results to be negligible.

One of the most important goals of this work is to analyze a possible connection between the Trojan fragments escaping from L_4, Centaurs and Jupiter-family comets. The existence of some genetic connection between the Trojan asteroids and the short-period comets was suggested by Hartmann et al. (1987),

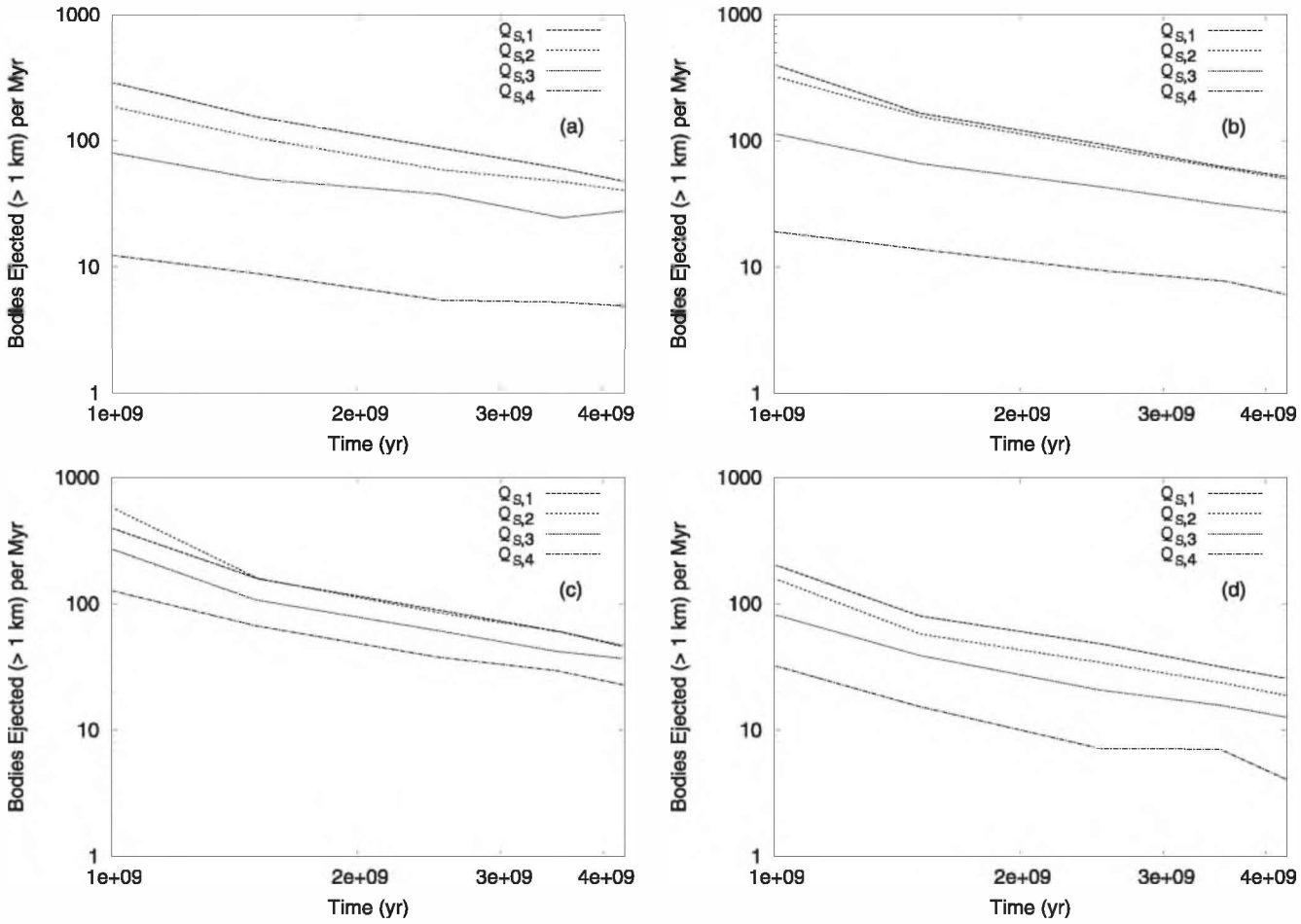

Fig. 7. Our estimates of the ejection rate of L_4 Trojans with diameters larger than 1 km per Myr obtained from the Q_S laws presented in Figs. 3a–d are shown in **a)–d)**, respectively.

Shoemaker et al. (1989), Jewitt & Luu (1990) and Fitzsimmons et al. (1994), who developed spectroscopic surveys and found similarities between comets and *D*-type asteroids, which are the most predominant among the Trojans. Recently, Di Sisto & Brunini (2007) analyzed the origin and distribution of the Centaur population. These authors inferred that the Scattered Disk Objects are probably the main source of Centaurs providing a current rate of $\sim 4 \times 10^6$ objects per Myr with a radius R greater than 1 km. Moreover, their results indicate that 30% of the Scattered Disk Objects entering the Centaur zone reach the region interior to Jupiter's orbit, obtaining a current rate of $\sim 1 \times 10^6$ Jupiter-family comets per Myr with a radius $R > 1$ km. In order to study the contribution of the Trojans to the current populations of Centaurs and Jupiter-family comets, we estimate a mean ejection rate of Trojan fragments from L_4 for every of our simulations over the last 500 Myr of evolution, where the number of bodies removed per unit time is more or less constant and the data sample results to be statistically significant. One of our main findings is that the maximum ejection rate corresponding to the smallest gaps between Q_S and Q_D is of ~50 objects larger than 1 km of diameter per Myr from the L_4 swarm, which results to be very much less than that obtained by Marzari et al. (1997), who derived a collisional ejection rate of ~3600 objects in the 1 to 40 km diameter range per Myr from L_4. According to our results, we would expect a maximum number of 1 Centaur or Jupiter-family comet with a diameter $D > 1$ km every 20 000 years from the L_4 Trojan swarm, while the estimates of Di Sisto & Brunini (2007) suggest the injection of 4 Centaurs and 1 Jupiter-family comet with a radius $R > 1$ km every year from the Scattered Disk. From this, we conclude that the contribution of the Trojan asteroids to the current populations of Centaurs and Jupiter-family comets is negligible.

5.4. Robustness of results

The results shown in this paper have been obtained using the stability and instability niches defined in Sect. 3, which present widths of 0.02 AU, 0.0125 and 2.25° in semimajor axis a, eccentricity e and inclination i, respectively. In order to test the dependence of our results on the size of those niches, we carry out several numerical experiments increasing the widths of such regions in a, e and i, which leads to magnify the stability region. In general terms, the larger the area of niches, the smaller the ejection rate of Trojan fragments from the L_4 swarm. In this work, we select small size niches in order to minimize the influence of the isolated Trojans in the distribution of the population. On the other hand, we find that the results concerning the L_4 size distribution and the formation of Trojan families are not sensitive to the size of the stability and instability regions constructed to developed our dynamical treatment.

At the same way, we also perform some numerical simulations in order to explore the sensitivity of our results to the initial population. To do this, we construct different initial size distributions (see Sect. 4.1) covering all the possibilities from a

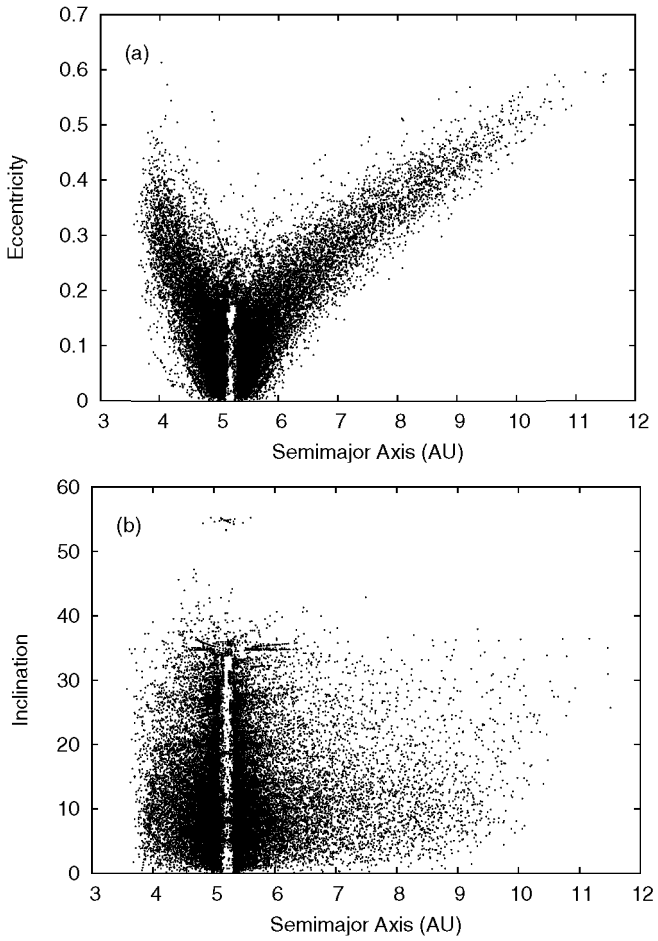

Fig. 8. Representative values of semimajor axis, eccentricity and inclination for the Trojan asteroids ejected from L_4.

small to a large initial Trojan mass. In particular, Fig. 9 shows a comparative analysis of results obtained from initial populations with 8 and 1000 times the current L_4 Trojan swarm mass (of order 5×10^{23} g (Jewitt et al. 2000)) and using the $Q_{S,1}$ law presented in Fig. 3b. We conclude that the size distribution of the L_4 Trojans, their mean collisional lifetimes, the current ejection rate of fragments from L_4 and the formation of families do not depend strongly on the initial mass of the population.

Finally, it is worth reminding the reader that the results presented in this work have been derived generating initial values of semimajor axis a, eccentricity e and inclination i from the distribution of L_4 Trojans shown in Fig. 1. In order to test the dependence of our results on the initial orbital distribution, we develop several simulations starting with a dynamically cold population, with eccentricities and inclinations smaller than 0.05 and 10°, respectively. Such e and i limit values are chosen arbitrary. Our outcomes show that $D \geq 1$ km Trojan fragments require time scales of order 100 Myr to reach the current dynamical configuration (see Fig. 10), while the smaller fragments occupy the stability niches very quickly, in only some thousands of years. In addition, we find that the results concerning the size distribution of the L_4 Trojans, their collisional lifetimes, the ejection rate of fragments from the L_4 swarm and the formation of families do not show a strong dependence on the initial distribution of orbital elements. From this analysis, we infer that the current orbital distribution of the Trojan asteroids does not offer a strong constraint on the dynamical origin of this population.

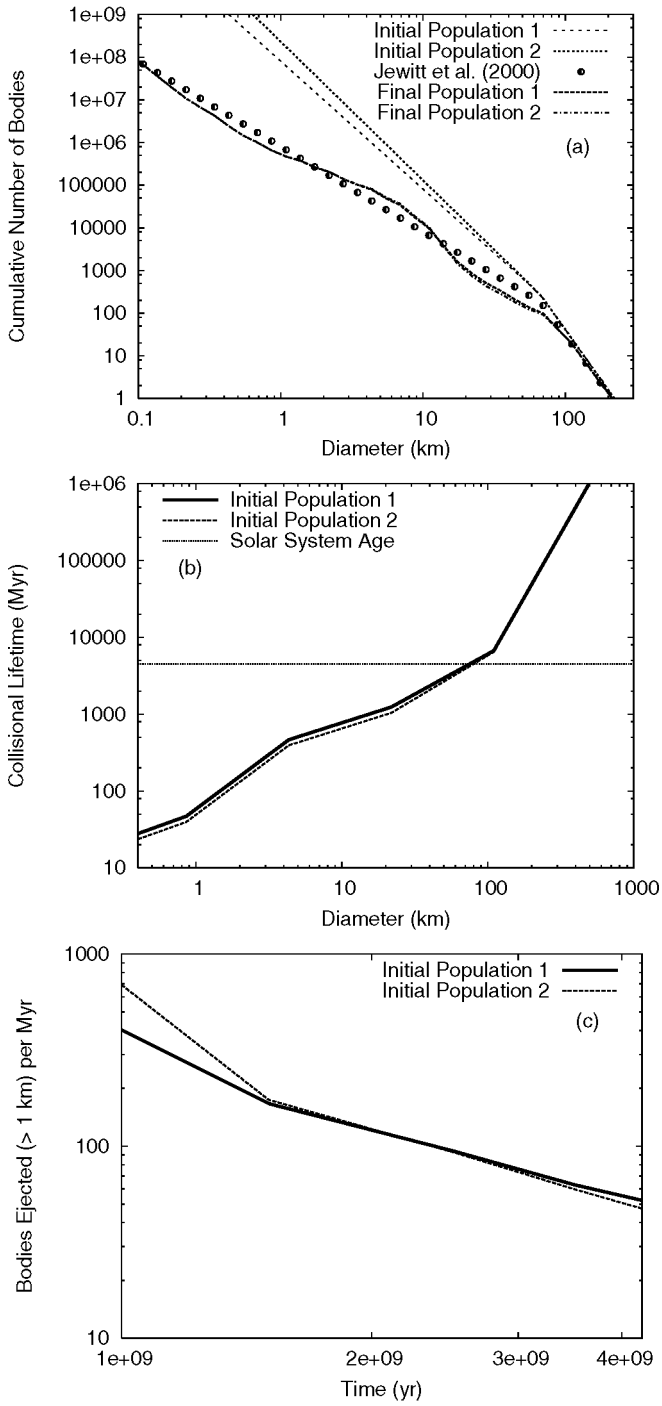

Fig. 9. Comparative analysis of results concerning the size distribution of the L_4 Trojans **a)**, their mean collisional lifetimes **b)** and the ejection rate of fragments from the L_4 swarm **c)**. The Initial Populations 1 and 2 refer to starting size distributions with 8 and 1000 times the current L_4 Trojan swarm mass, respectively.

6. Conclusions

We have presented a new study aimed at analyzing the collisional and dynamical evolution of the L_4 Trojan asteroids. The numerical code developed by de Elía & Brunini (2007) has been used, including a new dynamical treatment that takes into account the stability and instability regions of such swarm. As for the collisional parameters, we test different shattering impact specific energies Q_S and use a factor f_{ke} depending on target

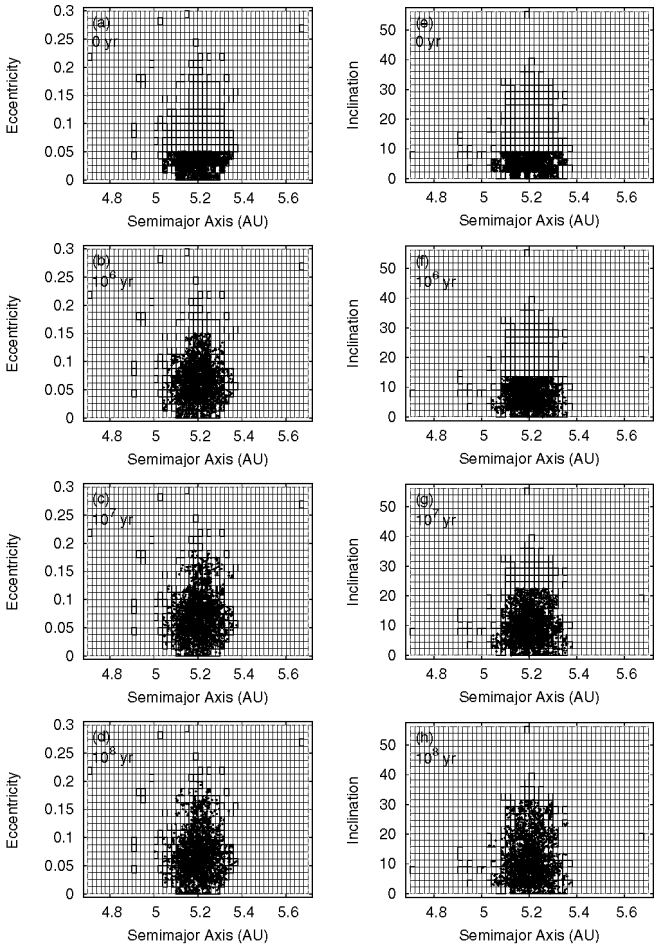

Fig. 10. Distribution of $D \geq 1$ km Trojan fragments with respect to semimajor axis a, eccentricity e and inclination i as a function of time.

size (Davis et al. 1995; O'Brien & Greenberg 2005) which are combined to yield the dispersing impact specific energy Q_D formulated by Benz & Asphaug (1999) for icy targets and 3 km s^{-1} impact velocity. The main conclusions obtained from this study are the following:

- Our estimates of the L_4 Trojan cumulative size distribution show waves that propagate from diameters of ~0.1 to ~80 km around of the values derived by Jewitt et al. (2000) from optical surveys. In general terms, we find that the largest gaps between Q_S and Q_D laws lead to the largest wave amplitudes.
- The results concerning the mean collisional lifetimes of the L_4 population indicate that the large Trojan asteroids have likely survived unaltered by catastrophic fragmentation events over the age of the Solar System, which is consistent with that discussed by Davis & Weidenschilling (1981) and Marzari et al. (1997).
- In order to compare our results concerning the L_4 Trojan families to those derived by by Beaugé & Roig (2001), Dotto et al. (2006) and Fornasier et al. (2007) from spectroscopic and photometric surveys, we analyze the formation of families from the breakup of bodies with diameters larger than 50 and 100 km that disperse fragments smaller than 40 km. Simulations with the largest gaps between Q_S and Q_D laws do not form any of such families over the age of the Solar System. On the other hand, most numerical experiments with the smallest gaps between Q_S and Q_D lead to the collisional disruption of 2 objects larger than 100 km in diameter but do not produce formation of families from parent bodies in the 50 to 100 km diameter range. In particular, the obtained results using the $Q_{S,1}$ law from Fig. 3b are consistent with the number of L_4 Trojan families found in the literature, also suggesting that new families might be identified in the future.
- One of the most important results obtained from our numerical experiments is that the maximum ejection rate of Trojan fragments from the L_4 swarm corresponding to the smallest gaps between Q_S and Q_D laws is of ~50 objects larger than 1 km of diameter per Myr, which results to be significantly less than that obtained by Marzari et al. (1997), who derived a collisional ejection rate of ~3600 objects in the 1 to 40 km diameter range per Myr from the same swarm. From our results, a maximum number of 1 Centaur or Jupiter-family comet with a diameter $D > 1$ km would be expected every 20 000 years from the L_4 Trojan swarm. Since the work developed by Di Sisto & Brunini (2007) suggests that 4 Centaurs and 1 Jupiter-family comet with a radius $R > 1$ km come from the Scattered Disk every year, we conclude that the contribution of the Trojan asteroids to the current populations of Centaurs and Jupiter-family comets is negligible.
- Finally, we infer that the current orbital distribution of the Trojan asteroids does not offer a strong constraint on the dynamical origin of this population.

Acknowledgements. This work was partially financed by ANPCyT by grant PICT 03-11044. We also acknowledge to Romina P. Di Sisto for valuable discussions during this work.

References

Beaugé, C., & Roig, F. 2001, Icarus, 153, 391
Benz, W., & Asphaug, E. 1999, Icarus, 142, 5
Bien, R., & Schubart, J. 1987, A&A, 175, 292
Binzel, R. P., & Sauter, L. M. 1992, Icarus, 95, 222
Brunini, A., & Fernández, J. A. 1999, Planet. Space Sci., 47, 591
Brunini, A., Di Sisto, R. P., & Orellana, R. B. 2003, Icarus, 165, 371
Campo Bagatin, A. 1998, Ph. D. Thesis, University of Valencia, Spain
Campo Bagatin, A., Cellino, A., Davis, D. R., Farinella, P., & Paolicchi, P. 1994, Planet. Space Sci., 42, 1079
Dahlgren, M. 1998, A&A, 336, 1056
Davis, D. R., & Weidenschilling, S. J. 1981, Lunar and Planetary Sci. XII, 199
Davis, D. R., Chapman, C. R., Weidenschilling, S. J., & Greenberg, R. 1985, Icarus, 63, 30
Davis, D. R., Weidenschilling, S. J., Farinella, P., Paolicchi, P., & Binzel, R. P. 1989, in Asteroids II ed. R. P. Binzel, T. Gehrels, & M. S. Matthews, (Tucson, USA: University of Arizona Press), 805
Davis, D. R., Ryan, E. V., & Farinella, P. 1994, Planet. Space Sci., 42, 599
Davis, D. R., Ryan, E. V., & Farinella, P. 1995, Lunar and Planetary Sci. Conf., 26, 319
de Elía, G. C., & Brunini, A. 2007, A&A, 466, 1159
Dell'Oro, A., & Paolicchi, P. 1998, Icarus, 136, 328
Dell'Oro, A., Paolicchi, P., Marzari, F., Dotto, E., & Vanzani, V. 1998, A&A, 339, 272
Dell'Oro, A., Marzari, F., Paolicchi, P, & Vanzani, V. 2001, A&A, 366, 1053
Di Sisto, R. P., & Brunini, A. 2007, Icarus, 190, 224
Dobrovolskis, A. R., & Burns, J. A. 1984, Icarus, 57, 464
Dotto, E., Fornasier, S., Barucci, M. A., et al. 2006, Icarus, 183, 420
Durda, D. D., Greenberg, R., & Jedicke, R. 1998, Icarus, 135, 431
Érdi, B. 1978, Celestial Mechanics, 18, 141
Farinella, P., Paolicchi, P., & Zappalà, V. 1982, Icarus, 52, 409
Fernández, J. A., Tancredi, G., Rickman, H., & Licandro, J. 1999, A&A, 352, 327
Fitzsimmons, A., Dahlgren, M., Lagerkvist, C. I., Magnusson, P., & Williams, I. P. 1994, A&A, 282, 634
Fornasier, S., Dotto, E., Marzari, F., Barucci, M. A., Boehnhardt, H., et al. 2004, Icarus, 172, 221
Fornasier, S., Dotto, E., Hainaut, O., et al. 2007, Icarus, in press

Fujiwara, A., & Tsukamoto, A. 1980, Icarus, 44, 142
Fujiwara, A., Kamimoto, G., & Tsukamoto, A. 1977, Icarus, 31, 277
Gault, D. E., Shoemaker, E. M., & Moore, H. J. 1963, NASA Tech. Note D-1767
Gil-Hutton, R., & Brunini, A. 2000, Icarus, 145, 382
Greenberg, R., Hartmann, W. K., Chapman, C. R., & Wacker, J. F. 1978, Icarus, 35, 1
Hartmann, W. K. 1988, Lunar and Planetary Sci. Conf., 19, 451
Hartmann, W. K., Tholen, D. J., & Cruikshank, D. P. 1987, Icarus, 69, 33
Holsapple, K. A. 1993, Annu. Rev. Earth Planet. Sci., 21, 333
Housen, K. R., & Holsapple, K. A. 1990, Icarus, 84, 226
Housen, K. R., & Holsapple, K. A. 1999, Icarus, 142, 21
Jewitt, D. C., & Luu, J. X. 1990, AJ, 100, 933
Jewitt, D. C., Trujillo, C. A., & Luu, J. X. 2000, AJ, 120, 1140
Lagrange, J.-L. 1772, Prix de l'Académie Royale des Sciences de Paris, Tome IX; reprinted in 1873, Oeuvres de Lagrange, Tome sixième, ed. J.-A. Serret (Paris: Gauthiers-Villars), 229
Levison, H., Shoemaker, E. M., & Shoemaker, C. S. 1997, Nature, 385, 42
Love, S. G., & Ahrens, T. J. 1996, Icarus, 124, 141
Marzari, F., Farinella, P., & Vanzani, V. 1995, A&A, 299, 267
Marzari, F., Scholl, H., & Farinella, P. 1996, Icarus, 119, 192
Marzari, F., Farinella, P., Davis, D. R., Scholl, H., & Campo Bagatin, A. 1997, Icarus, 125, 39
Marzari, F., Scholl, H., Murray, C., & Lagerkvist, C. 2002, in Asteroids III, ed. W. F. Bottke, A. Cellino, P. Paolicchi, & R. P. Binzel (Tucson, USA: University of Arizona Press), 725
Marzari, F., Tricarico, P., & Scholl, H. 2003, Icarus, 162, 453
Melosh, H. J. 1989, Oxford Monographs on Geology and Geophysics (New York: Oxford University Press), 11
Melosh, H. J., & Ryan, E. V. 1997, Icarus, 129, 562
Milani, A. 1993, Celest. Mech. Dyn. Astron., 57, 59
Milani, A. 1994, Asteroids, Comets, Meteors 1993: Proceedings of the 160th International Astronomical Union, Belgirate, Italy, ed. A. Milani, M. Di Martino, & A. Cellino, International Astronomical Union. Symposium No. 160 (Dordrecht: Kluwer Academic Publishers), 159
Nakamura, A., & Fujiwara, A. 1991, Icarus, 92, 132
O'Brien, D. P., & Greenberg, R. 2003, Icarus, 164, 334
O'Brien, D. P., & Greenberg, R. 2005, Icarus, 178, 179
Petit, J., & Farinella, P. 1993, Celest. Mech. Dyn. Astron., 57, 1
Rabe, E. 1967, AJ, 72, 10
Ryan, E. V. 1992, Ph. D. Thesis, University of Arizona, Tucson, USA
Schubart, J., & Bien, R. 1987, A&A, 175, 299
Shoemaker, E. M., Shoemaker, C., & Wolfe, R. F. 1989 in Asteroids II, ed. R. P. Binzel, T. Gehrels, & M. S. Matthews (Tucson, USA: University of Arizona Press), 487
Stoeffler, D., Gault, D. E., Wedekind, J., & Polkowski, G. 1975, J. Geophys. Res., 80, 4062
Szebehely, V. 1967 (New York: Academic Press)
Tedesco, E. F. 1989, in Asteroids II, ed. R. P. Binzel, T. Gehrels, & M. S. Matthews (Tucson, USA: University of Arizona Press), 1090
Vokrouhlický, D., Brož, M., Bottke, W. F., Nesvorný, D., & Morbidelli, A. 2006, Icarus, 182, 118
Yoshida, F., & Nakamura, T. 2005, AJ, 130, 2900